Pre-low noise amplifier (LNA) filtering linearisation method for low-power ultra-wideband complementary metal oxide semiconductor LNA

Mohammed Nadhim Abbas, Farooq Abdulghafoor Khaleel

Department of Electrical Engineering, University of Baghdad, Al-Jadriya district, Baghdad, Iraq
E-mail: Mohammed.nadhim@uob.edu.iq

Published in *The Journal of Engineering*; Received on 10th January 2018; Accepted on 20th March 2018

Abstract: This study describes the use of a pre-low noise amplifier (LNA) third-order notch filter as a novel linearity enhancement technique for ultra-wideband complementary metal oxide semiconductor LNA current-reuse topology. The second/third order input intercept point (IIP2/3) has improved along the entire working bandwidth (BW) from 2.1 to 12.5 GHz. The suggested linearisation technique achieves maximum/minimum IIP2 improvement from 19.068 to 104.143 dBm at 6.4 GHz and from 22.5 to 57.42 dBm at 5.5 GHz, respectively. In addition, this work achieves maximum/minimum IIP3 improvement from −7.956 to 34.688 dBm at 6.4 GHz and from −9.986 to 8.281 dBm, respectively. Moreover, the suggested linearisation technique does not affect the total ultra-wideband (UWB)-LNA power consumption, which is only 6.7 mW. Furthermore, the linearised UWB-LNA average noise figure is 1.6535 dB at the entire working BW. The simulation is performed and optimised with an advanced design system utilising BSIM3v3 TSMC 180 nm model files at different temperature values.

1 Introduction

The Federal Communications Commission standardised the frequency spectrum ranging from 2.1 to 12.5 GHz for too many ultra-high-frequency and super-high-frequency applications, such as satellite communications, industrial, scientific, and medical band communications, and ultrawideband (UWB) communications. The plethora of radio frequency (RF) applications' standards negatively affect the aforementioned frequency spectrum with strong interferers, such as WiMAX, 2.4/5.8 GHz Wi-Fi, UWB, ZigBee, GSM etc. Consequently, enhancing the performance of the UWB receivers emerged as a promised research field to support and sense multiple RF applications' standards with optimum performance characteristics [1].

The most stringent and challenging building block of a UWB receiver is the UWB low noise amplifier (UWB-LNA). To achieve high-receiver performance, the UWB-LNA must meet many critical design criteria, such as low-noise figure (NF), high-flat gain, and low-input/output return losses over the entire working bandwidth (BW) while consuming low power in deep submicron scaling. In addition, another critical design challenge is to attain high linearity over the operating BW. That is, too many high power in-band interferers and intermodulation (IM) terms enter the UWB transceiver, which compromises the sensitivity of the overall UWB receiver. The second and third orders are the most important IM terms. Their high power can significantly deteriorate the sensitivity of the overall UWB receiver system. The high power of the second-order IM term, which is generated at a frequency equivalent to the difference of the two interferers' frequency components, greatly affects and destroys the desired low-frequency RF input signal and the mixer operation. On the other hand, the high power third-order IM term can deteriorate the sensitivity or block other desired applications' signals in the working BW [2].

General LNA linearisation techniques were reported in detail in [2]. However, most of the reported linearisation techniques neglected second order input intercept point (IIP2) improvement studied the linearisation of narrowband applications and aimed to mitigate the levels of the IM terms after their generation by the LNA. Pre-LNA linearisation techniques aimed to enhance the linearity by introducing methods to compensate the IM terms before they enter the LNA.

The pre-linearisation method of the narrowband 5 GHz, 130 nm complementary metal oxide semiconductor (CMOS) LNA using the transformer feedback method was discussed in [3]. The simulation results showed a high-power consumption of 15.4 mW and +10 dBm third order input intercept point (IIP3) improvement from 9.4 to 19.7 dBm. However, the previously reported pre-distortion linearisation scheme implementing an RF transformer was limited by the difficulty of implementing such transformers in RF integrated circuits and the transformer's requirement for a very large die area to implement. Furthermore, the previously reported work had limited sweet spot and was very sensitive to bias voltages of the pre-distorter circuit. In addition, the mutual coupling was affected by inductor values' deviations. Consequently, IIP3 values might deteriorate.

A recent study [4] on pre-distortion linearisation technique in the LNA's input matching circuit proposed a linearisation technique that mitigated the effect of the non-linearity components generated by the input matching circuit utilising a weakly inverted auxiliary transistor. However, the resultant IIP3 was 11 dBm, the operating BW ranged from 0.3 to 2.96 GHz, and the effect of the used linearisation technique on IIP2 improvement was not mentioned.

Another recent study on pre-distortion linearisation technique for UWB-LNA operating from 0.8 to 10.4 GHz was discussed in [5]. The simulation results showed an IIP3 improvement to 13 dBm, a minimum NF of 3 dB, and the circuit consumed 7.2 mW.

In this study, the third-order notch filter described in [6] is used as a novel pre-LNA linearisation method to improve the linearity of the UWB-LNA current reuse topology described in [7]. Mathematical analysis shows that both IIP2 and IIP3 achieve good values over the entire working BW. In Section 2, the proposed linearisation technique to improve the linearity of the UWB-LNA is discussed. Section 3 shows the simulation data that verifies the proposed IIP2/3 improvement technique. Finally, Section 4 concludes the paper.

2 Design methodology

When two input frequencies with small frequency spacing between them enter the UWB-LNA, which is usually a non-linear system, the second-order and third-order IM products are generated. Consequently, if the power of the IM products is high, then the IM products will corrupt other applications' frequencies in the working BW. The generated third-order IM components are shown in Fig. 1*a* and their amplitude can be written as follows [8]:

$$\frac{3\alpha^3 A_1^2 A_2}{4}\cos(2\omega_1 - \omega_2)t, \tag{1a}$$

$$\frac{3\alpha^3 A_2^2 A_1}{4}\cos(2\omega_2 - \omega_1)t, \tag{1b}$$

where $A_{1,2}$are the amplitudes of the two-tone interferers at ω_1 and ω_2, respectively.

If the amplitude of one of the two-tone interferers at ω_1 and ω_2 is filtered-out before the interferer enters the UWB-LNA, then the generated third-order IM component generated by the filtered interferer is much lower than the third-order IM component generated before filtering. For example, Fig. 1*b* shows that the filtered interferer power at (f_1) generates much less third-order IM power at ($2f_1$–f_2) before the interferer filtering as shown in Fig. 1*a* as (1a) implies. Consequently, the desired RF signal at ($2f_1$–f_2) suffers from negligible interference generated by the reduced third-order IM product.

The second-order IM products generated by two closely frequency spacing interferers entering the UWB-LNA are shown in Fig. 2*a*.

The same derivation for the amplitude of the third-order IM products can be carried for the amplitude of the second-order IM products and the resultant amplitudes are

$$\left(\alpha_2 A_1 A_2 + \frac{3}{2}\alpha_4 A_1^3 A_2 + \frac{3}{2}\alpha_4 A_2^3 A_1\right)\cos((\omega_2 - \omega_1)t), \tag{2a}$$

$$\left(\alpha_2 A_1 A_2 + \frac{3}{2}\alpha_4 A_1^3 A_2 + \frac{3}{2}\alpha_4 A_2^3 A_1\right)\cos((\omega_1 + \omega_2)t). \tag{2b}$$

In direct-conversion RF receivers, the most important second-order IM term is at (ω_2–ω_1) because this IM term is very close to the RF

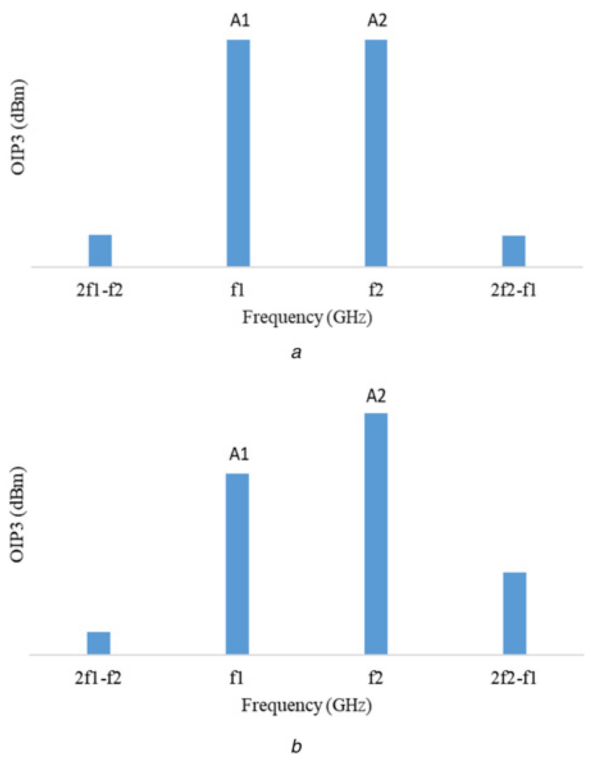

Fig. 1 *Third-order IM products*
a Generated
b Reduced

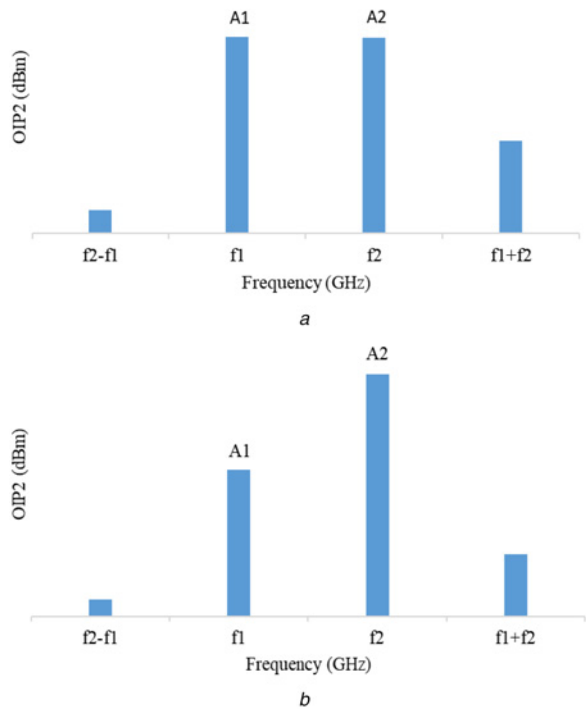

Fig. 2 *Second-order IM products*
a Generated
b Reduced

input signal frequency and consequently high-power IM term corrupts the desired RF input signal. If the interferer power at f_1 is reduced before entering the UWB-LNA, then the generated second-order IM product is much lower than that before mitigation (filtering) as (2) implies and this can be shown in Fig. 2*b*.

The third-order notch filter is used to filter out the interferer's power at f_1 by tuning the filter's cutoff frequency to f_1. The third-order notch filter is connected to the input matching circuit of the low power UWB-LNA as shown in Fig. 3. This connection assures that the unwanted interferer power is filtered-out before the second and third IM products are generated by Q1.

The input impedance, cutoff frequency, and passing frequency for the third-order notch filter can be written as (3), respectively [6]

$$Z_{\text{in}}(S) = \frac{L_1(C_1 + C_2)S^2 + 1}{C_1 \cdot C_2 \cdot L_1 \cdot S^3 + C_1 \cdot S}, \tag{3a}$$

$$\omega_{\text{cutoff}} = \frac{1}{\sqrt{L_1(C_1 + C_2)}}, \tag{3b}$$

$$\omega_{\text{passing}} = \frac{1}{\sqrt{L_1 C_1}}. \tag{3c}$$

Although the practical implementation is missing; however, to tune the filter to the desired interferer frequency, a multi-tap RF spiral inductor can be implemented to realise different inductor values over the working BW. Moreover, a variable active-inductor is another option to be followed as a future work for this study.

The third-order filter's input impedance is very low at the desired interferer frequency. Consequently, the interferer signal power is significantly diminished (sinked) by the filter's low impedance value near zero (ground). Moreover, the third-order notch filter resonates with the input matching circuit (L_s and C_{in}) for the UWB-LNA and consequently yields the input return losses to be around 0 dB at the interferer frequency. However, the third-order notch filter provides very sharp cutoff response and the other

doi: 10.1049/joe.2018.0043

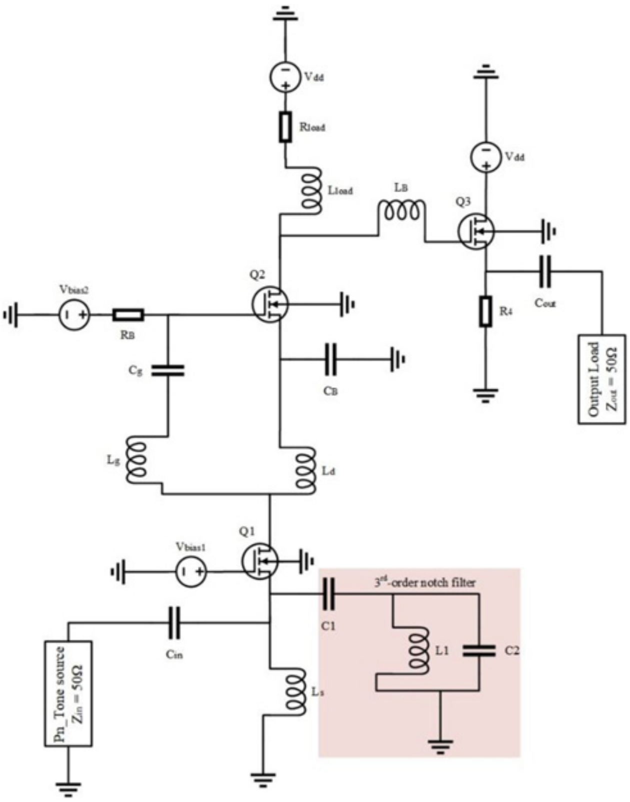

Fig. 3 *Proposed linearisation technique*

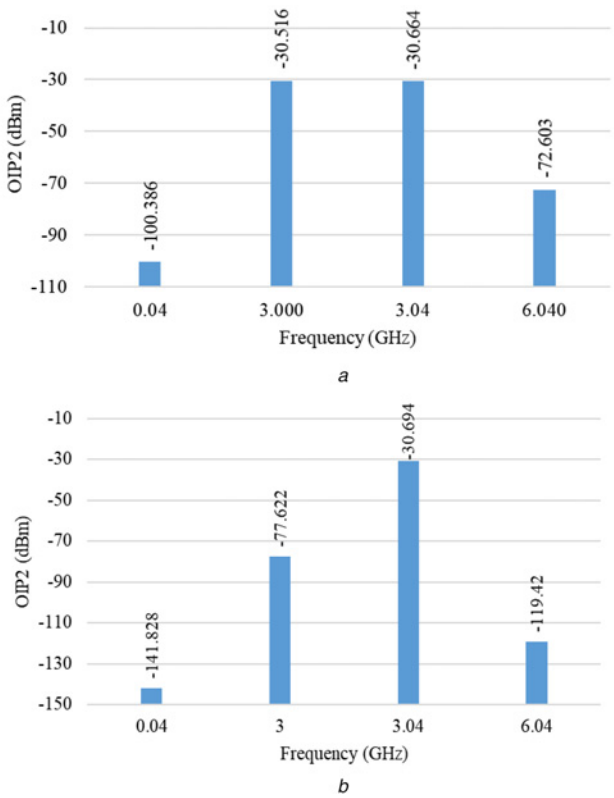

Fig. 4 *OIP2*
a Before linearisation
b After linearisation

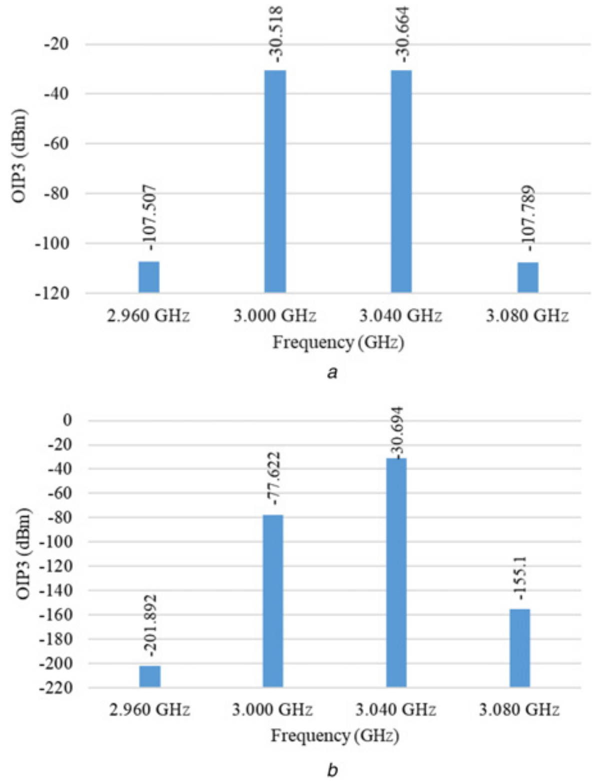

Fig. 5 *OIP3*
a Before linearisation
b After linearisation

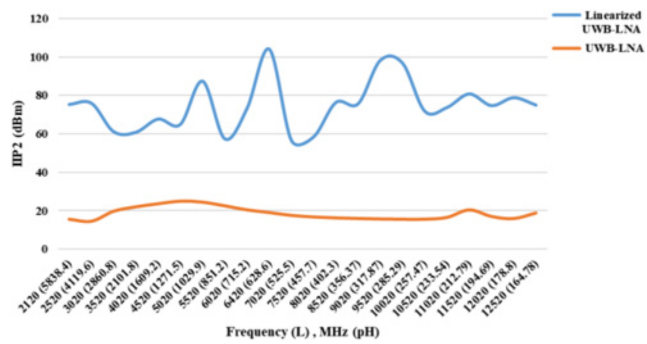

Fig. 6 *Linearised IIP2 versus conventional IIP2*

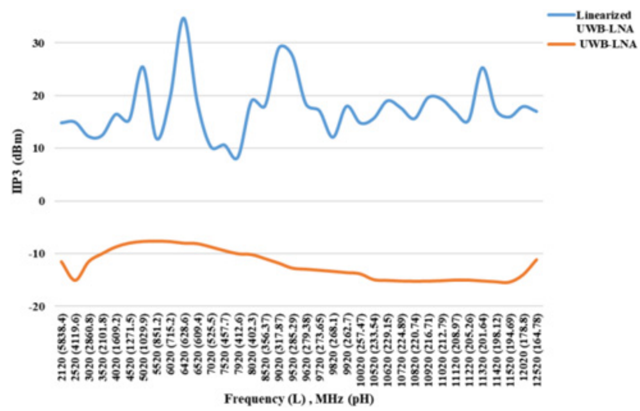

Fig. 7 *Linearised IIP3 versus conventional IIP3*

Table 1 IIP2/3 improvement versus temperature variation

	Temperature frequency, GHz	−40°C	25°C	90°C
IIP3, dBm (before/after)	3	(−11.913/10.994)	(−11.505/12.203)	(−11.376/13.096)
	6	(−7.57/18.993)	(−7.655/19.523)	(−7.514/20.248)
	10	(−13.619/14.707)	(−13.817/14.785)	(−13.159/15.878)
IIP2, dBm (before/after)	3	(20.918/60.417)	(19.722/61.134)	(18.045/61.536)
	6	(22.321/72.698)	(20.42/73.192)	(18.254/73.536)
	10	(14.756/70.499)	(15.686/71.774)	(16.775/73.393)

signals in the frequency spectrum occurs at frequency locations that the UWB-LNA has sufficient input return losses ($S_{11} < -10$ dB) and high gain. This will be elaborated more in Section 3.

3 Simulation results

The performance of the proposed linearisation technique is validated through the design and simulation the UWB-LNA along with the third-order notch filter using 180 nm TSMC CMOS BSIM3v3 model files and the Advanced Design System (ADS2016.01) software. The main goal is to improve the IIP2 and IIP3 values for the UWB-LNA topology using the proposed linearisation technique. In addition, the proposed linearisation technique does not affect the UWB-LNA's total low power consumption, which is only 6.7 mW including the Q3 output stage.

The IIP2/3 measurement from the two-tone test can be written from second/third order output intercept point (OIP2/3), respectively, as (4) [8]

$$\text{IIP2} = P_{\text{int}} - P_{\text{IM}} + P_{\text{in}}, \quad (4a)$$

$$\text{IIP3} = \frac{P_{\text{int}} - P_{\text{IM}}}{2} + P_{\text{in}}, \quad (4b)$$

where P_{int} is the interferer power, P_{IM} is the IM product power, and P_{in} is the input power. The input power of the interferers is chosen to be −50 dBm with a frequency spacing of 40 MHz between them. Consider, for example, that the two input interferer frequencies are 3 and 3.04 GHz, respectively, and the third-order notch filter is tuned to attenuate the interferer power at 3 GHz, then the resultant IIP2 before and after linearisation are 19.722 and 61.134 dBm as shown in Figs. 4*a* and *b*, respectively. Moreover, the IIP3 values before and after linearisation are −11.51 and 12.135 dBm as shown in Figs. 5*a* and *b*, respectively. Since the second IM term occurs outside the working band of the UWB-LNA at (f_2–f_1), therefore, it has low amplitude. However, this IM term may distort the required low-frequency RF input signal and generates undesired harmonics affecting the mixer operation.

Figs. 4 and 5 show that the generated second/third-order IM terms have the much low power of −141.828 dBm at f_2–f_1 (40 MHz) and −201.892 dBm at $2f_1$–f_2 (2.96 GHz), respectively. Consequently, this leads to much less distortion and increased receiver sensitivity if the desired RF signal occurs at 40 MHz or 2.69 GHz.

The two-tone test is swept over the working −3 dB BW ranging from 2.1 to 12.5 GHz and the resultant IIP2/IIP3 values over the working BW are shown in Figs. 6 and 7, respectively.

Fig. 6 shows a minimum IIP2 improvement of 35 dBm at 5.52 GHz and maximum IIP2 improvement of 85.1 dBm at 6.42 GHz. On the other hand, Fig. 7 shows a minimum IIP3 improvement of 18.3 dBm at 7.92 GHz and a maximum IIP3 improvement of 42.6 dBm at 6.42 GHz. Further IIP2/3 improvement can be achieved by fine tuning the filter's inductor value.

The proposed linearisation technique does not include temperature-dependent active devices and hence the linearisation improvement is constant over temperature variations. Table 1 shows the IIP2/3 improvement over temperature variation.

The filter sharp response provides the desired interferer signal attenuation. In addition, the filter response provides the BW flat gain for the other interferer signal although both interferer signals have

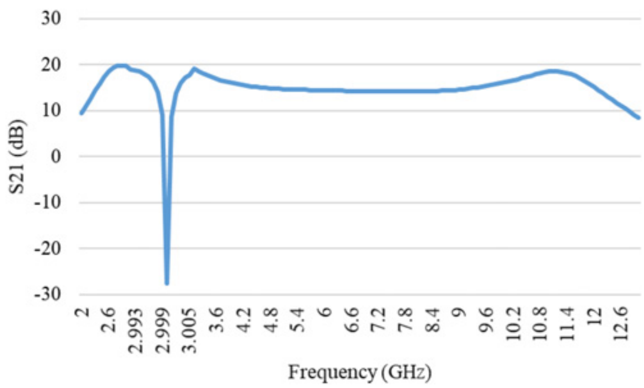

Fig. 8 *Filter's sharp response effect on the gain*

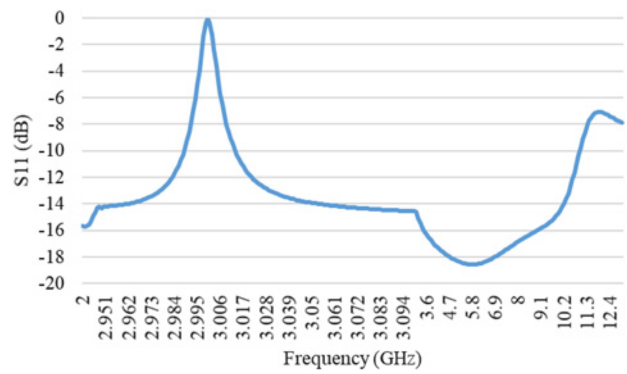

Fig. 9 *Filter's response effect on S_{11}*

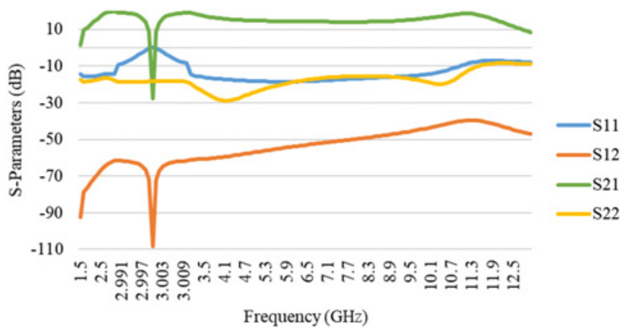

Fig. 10 *Linearised UWB-LNA S-parameters*

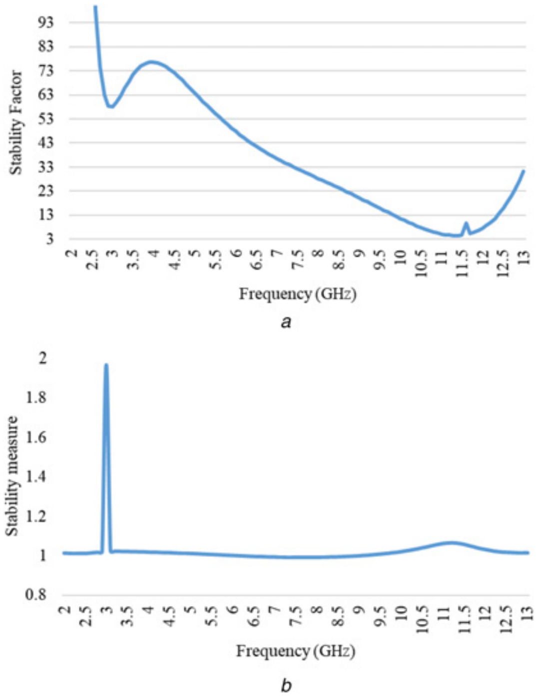

Fig. 11 *Linearised UWB-LNA stability conditions*
a Stability factor
b Stability measure

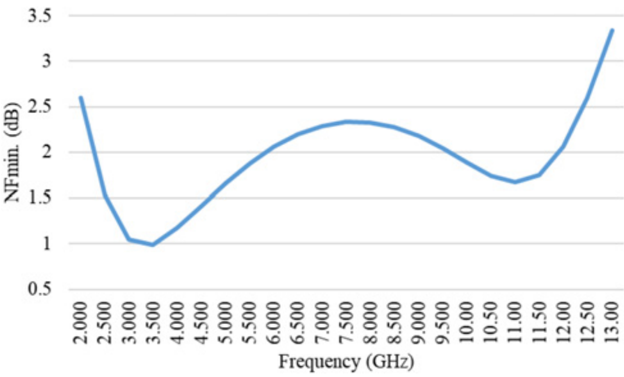

Fig. 12 *Linearised UWB-LNA NF*

narrow frequency spacing. This can be illustrated as shown in Fig. 8.

Consider two interferer signals at 3 and 3.04 GHz and the desired rejected interferer is at 3 GHz. The filter's response provides enough attenuation response for the interferer signal at 3 GHz. In addition, the filter's response provides enough gain for the other interferer signal at 3.04 GHz as shown in Fig. 8. Moreover, the input insertion losses at 3 GHz increases to 0 dB because of the filter's low impedance at this frequency, however, the sharp filter's response provides low enough input return losses (<−10 dB) for the other interferer signal at 3.04 GHz as shown in Fig. 9.

The linearised UWB-LNA provides enough output return loss below −10 dB over the entire working BW. In addition, reverse isolation is below −40 dB over the entire working BW as shown in Fig. 10.

The simulated stability factor and stability measure are calculated based on the S-parameters shown in Fig. 10 as an indication of the linearised UWB-LNA stability. It is shown in [9] that a stability factor over unity and non-negative stability measure are the two necessary and sufficient conditions for unconditional UWB-LNA stability if S_{12} is a very low value (the UWB-LNA has sufficient reverse isolation) as shown in (5) and Fig. 11

$$k\left(\text{stability factor}\right) = \frac{1 - \left|S_{11}\right|^2 - \left|S_{22}\right|^2 + \left|S_{11} \times S_{22} - S_{12} \times S_{21}\right|^2}{2 \times \left|S_{12} \times S_{21}\right|}, \tag{5a}$$

$$b\left(\text{stability measure}\right) = 1 + \left|S_{11}\right|^2 - \left|S_{22}\right|^2 - \left|S_{11} \times S_{22} - S_{12} \times S_{21}\right|^2. \tag{5b}$$

The linearised UWB-LNA achieves a minimum NF of 0.97 dB at 3.3 GHz and a maximum NF of 2.3 dB at 7.72 dB and hence the calculated average NF is 1.6 dB over the working BW as shown in Fig. 12

$$\text{FOM} = \frac{\text{Gain}^{\,(\text{linear})} \times \text{IIP3}^{\text{mW}} \times \text{BW}^{\text{GHz}}}{P_{\text{dc}}^{\text{mW}} \times \left(\text{NF}^{(\text{linear})} - 1\right)}. \tag{6}$$

Table 2 compares the performance of the proposed linearisation technique with other recently published UWB-LNAs and pre-distortion linearisation techniques. The figure of merit (FOM) as [4] suggested is used as a measure for comparison.

Table 2 Performance comparison of the proposed linearisation technique with other state-of-the-art LNAs

Ref.	Publication year	Technology, nm	BW, GHz	Voltage gain, dB	NF, dB	Power, mW	IIP2, dBm	IIP3, dBm	FOM
[this work][a]	—	180	2.1–12.5	14.1	1.6	6.7	54.8–104.14	8.3–34.7	2471.13
[3][a], n	2006	130	5	11.6	1.15	15.3	N.A	9.4	35.7
[10][a]	2010	90	0.5–3	20.1	2.32	5.5	N.A	−1	5.2
[11][a]	2009	130	2.8	12.1	12.3	3.2	60	18.5	15.5
[4][a]	2017	180	0.3–2.96	18.55	2.7	4.15	N.A	11	79.2
[5][a]	2017	180	0.8–10.4	13.7	3	7.2	27–32	13	129.1
[12][a]	2015	130	2.35–9.37	20.6	3.68	9.97	39	−4	2.3
[13][a]	2015	180	3.1–10.6	15.8	2.2	9	N.A.	−6	2
[14][a]	2015	180	2.8–10.1	13.7	2.5	4.1	22	9.5	95.1
[15][a]	2016	180	1–10.3	16	4.1	10.9	N.A.	11	43.2
[16][a]	2010	180	0.9–10	14	3.5	7.6	N.A.	1.8	28
[17][a]	2015	90	2.4–10.4	19	3.5	14.8	42.8	13.1	79.2
[18][a]	2016	90	3.1–10.6	15.3	1.21	13.5	N.A.	−3	5.1
[19][a]	2013	130	0.07–7.5	17.9	2.3	15.6	N.A.	13.1	109.7
[20][a]	2013	130	2.1–3.1	10	1.66	12	N.A.	11.1	7

[a]Simulation results. n, narrowband.

For a fair FOM comparison, the BW corresponds to −3 dB from maximum S_{21} and $S_{11} < -10$ dB, average NF over the working BW, minimum flat gain over BW neglecting gain peaking at the two BW sides, and average IIP3 over the working BW are considered through the (6) calculation. The proposed linearisation technique does not affect the UWB-LNA topology performance before and after linearisation in terms of power, gain, NF, and BW. In addition, the proposed linearisation technique provides IIP2/3 improvement independent of temperature variation.

A very high FOM measure due to high IIP3 average value. This high IIP3 value is due to the reduction of the interferer power before entering the UWB-LNA. Furthermore, the square relation in (1) further reduces the interferer level after passing the UWB-LNA and hence the spacing between the interferer level and the third-order IM component greatly enlarged and consequently a high IIP3 value is achieved.

4 Conclusion

The use of a third-order notch filter is used as a novel linearisation technique for UWB-LNA. The filter's component goal is to mitigate the interferer power before the interferers enter the non-linear metal oxide semiconductor field effect transistor device. The square and cubic relations of the second and third non-linear terms reduces further the interferer power to very low levels and hence improve the IIP2/3, respectively. In summary, high IIP2/3 values are achieved using the suggested technique with low power, good gain, and temperature variation resistivity, wide-flat BW with sufficient input and output return losses, and low minimum NF.

5 References

[1] F. C. Commission: 'FCC online table of frequency allocations', 2017. Available at https://www.fcc.gov/oet/spectrum/table/fcctable.pdf, accessed 21 September 2017

[2] Zhang H., Sánchez-Sinencio E.: 'Linearization techniques for CMOS low noise amplifiers: A tutorial', *IEEE Trans. Circuits Syst. I, Regul. Pap.*, 2011, **58**, (1), pp. 22–36

[3] Vitzilaios G., Papananos Y., Theodoratos G., *et al.*: 'Magnetic-feedback-based predistortion method for low-noise amplifier linearization', *IEEE Trans. Cicuits Syst.*, 2006, **53**, (12), pp. 1441–1445

[4] Jafarnejad R., Jannesari A., Sobhi J.: 'Pre-distortion technique to improve linearity of low noise amplifier', *Microelectron. J.*, 2017, **61**, (July 2016), pp. 95–105

[5] Jafarnejad R., Jannesari A., Sobhi J.: 'A linear ultra wide band low noise amplifier using pre-distortion technique', *AEUE – Int. J. Electron. Commun.*, 2017, **79**, pp. 172–183

[6] Samavati H., Rategh H.R., Lee T.H.: 'A 5-GHz CMOS wireless LAN receiver front end', *IEEE J. Solid-State Circuits*, 2000, **35**, (5), pp. 765–772

[7] Lee J.Y., Park H.K., Chang H.J., *et al.*: 'Low-power UWB LNA with common-gate and current-reuse techniques', *IET Microw. Antennas Propag.*, 2012, **6**, (7), pp. 793–799

[8] Razavi B.: 'RF microelectronics' (Prentice Hall, New Jersey, USA, 2011, 2nd edn.)

[9] Gonzalez G.: 'Microwave transistor amplifiers' (Prentice-Hall, Inc., New Jersey, USA, 1984, 1st edn.)

[10] Zare Fatin G.H., Koozehkanani Z.D., Sjöland H.: 'A technique for improving gain and noise figure of common-gate wideband LNAs', *Analog Integr. Circuits Signal Process.*, 2010, **65**, (2), pp. 239–244

[11] Nabavi A.: 'Improved derivative superposition scheme for simultaneous second- and third-order distortion cancellation in LNAs', *Electron. Lett.*, 2009, **45**, (25), pp. 1323–1325(2)

[12] Arshad S., Ramzan R., Muhammad K., *et al.*: 'A sub-10 mW, noise cancelling, wideband LNA for UWB applications', *AEU – Int. J. Electron. Commun.*, 2015, **69**, (1), pp. 109–118

[13] Wan Q., Wang Q., Zheng Z.: 'Design and analysis of a 3.1–10.6 GHz UWB low noise amplifier with forward body bias technique', *AEU – Int. J. Electron. Commun.*, 2015, **69**, (1), pp. 119–125

[14] Mohammadi I., Sahafi A., Sobhi J., *et al.*: 'A linear, low power, 2.5-dB NF LNA for UWB application in a 0.18um CMOS', *Microelectron. J.*, 2015, **46**, (12), pp. 1398–1408

[15] Sahafi A., Sobhi J., Koozehkanani Z.D.: 'Linearity improvement of gm-boosted common gate LNA: analysis to design', *Microelectron. J.*, 2016, **56**, (Supplement C), pp. 156–162

[16] Hu B., Yu X., He L.: '0.9–10 GHz low noise amplifier with capacitive cross coupling'. 2010 IEEE Int. Conf. on Ultra-Wideband, 2010, vol. 1, pp. 1–4

[17] Jafari B.M., Yavari M.: 'A UWB CMOS low-noise amplifier with noise reduction and linearity improvement techniques', *Microelectron. J.*, 2015, **46**, (2), pp. 198–206

[18] Pandey S., Kondekar P.N., Nigam K., *et al.*: 'A 0.9 V, 3.1–10.6 GHz CMOS LNA with high gain and wideband input match in 90 nm CMOS process'. 2016 IEEE Asia Pacific Conf. on Circuits and Systems (APCCAS), Jeju, South Korea, 2016, pp. 730–733

[19] Shirazi A.H.M., Rashtian H., Mirabbasi S.: 'A linearity enhancement technique and its application to CMOS wideband low-noise amplifiers'. 2012 19th IEEE Int. Conf. on Electronics, Circuits, and Systems (ICECS 2012), Seville, Spain, 2012, pp. 57–60

[20] Zafar F.: 'Design of a highly linear fully integrated wideband LNA in 0.13 μm CMOS technology'. 2013 10th Int. Conf. on Electrical Engineering, Computing Science and Automatic Control (CCE), Mexico City, Mexico, 2013, pp. 453–457